



## Study of Excited B-mesons

The DØ Collaboration  
URL: <http://www-d0.fnal.gov>  
(Dated: March 4, 2006)

Excited B mesons  $B_1$  and  $B_2^*$  are observed directly for the first time as two separate states in fully reconstructed decays to  $B^{+(*)}\pi^-$ . The mass of  $B_1$  is measured to be  $5720.8 \pm 2.5 \pm 5.3 \text{ MeV}/c^2$  and the mass difference  $\Delta M$  between  $B_2^*$  and  $B_1$  is  $25.2 \pm 3.0 \pm 1.1 \text{ MeV}/c^2$ . The production rate for  $B_J$  is calculated as a fraction  $16.5 \pm 2.4 \pm 2.8\%$  of the production rate of the  $B^+$  meson.

*Preliminary Results for Winter 2006 Conferences*

## 1. INTRODUCTION

To date, the spectroscopy of mesons containing  $b$ -quarks is not well studied. Only the ground stable  $0^-$  states  $B^+$ ,  $B_d^0$ ,  $B_s^0$  and the excited  $1^-$  state  $B^*$  are considered as established by the PDG [1]. The quark model predicts the existence of two wide ( $B_0^*$  and  $B_1^*$ ) and two narrow ( $B_1$  and  $B_2^*$ ) bound  $P$  states [2]. The wide states decay through the  $S$  wave and therefore have a large width of a few hundred  $\text{MeV}/c^2$ . Such states are difficult to distinguish from combinatoric background. The narrow states decay through the  $D$  wave ( $L = 2$ ) and therefore should have a small width of around  $10 \text{ MeV}/c^2$  [2–5].

Almost all observations of the narrow  $P$  states  $B_1$  and  $B_2^*$  have been made indirectly in inclusive or semi-inclusive decays [6–9], which prevents their separation and a precise measurement of their properties. The measurement of ALEPH [10], although partially done with exclusive  $B$  decays, was statistically limited and model dependent. The masses, widths and decay branching ratios of these states, in contrast, are predicted with good precision by various theoretical models [2–5].

These predictions can be verified experimentally, and such a comparison can provide important information on the quark interaction inside bound states, aiding further development of the non-perturbative QCD. This note presents the study of narrow  $L = 1$  states decaying to  $B^{+(*)}\pi$  with exclusively reconstructed  $B$  mesons using the statistics collected in the  $D\mathcal{O}$  experiment during 2002-2005 and corresponding to a total integrated luminosity of about  $1 \text{ fb}^{-1}$ .

## 2. DATA SAMPLE

### 2.1. $B^+$ Selection

$B_1$  and  $B_2^*$  mesons were reconstructed in the following decays [11]:

$$B_1^0 \rightarrow B^{*+}\pi^-; B^{*+} \rightarrow B^+\gamma \quad (1)$$

$$B_2^{*0} \rightarrow B^{*+}\pi^-; B^{*+} \rightarrow B^+\gamma \quad (2)$$

$$B_2^{*0} \rightarrow B^+\pi^- \quad (3)$$

The  $B^+$  mesons are reconstructed in the exclusive decay  $B^+ \rightarrow J/\psi K^+$  with  $J/\psi$  decaying to  $\mu^+\mu^-$ .

The  $D\mathcal{O}$  detector is described in detail elsewhere [12]. The muons were required to be identified with the standard  $D\mathcal{O}$  muon identification tools. In addition, the following selection criteria were applied. Both muons must have an associated track in the central tracking system with at least 2 measurements in the silicon microstrip tracker (SMT), and a transverse momentum  $p_T^\mu > 1.5 \text{ GeV}/c$  as measured in the central tracker including the SMT and central fiber tracker (CFT). At least one of the two muons should have hits in all 3 layers of muon chambers. The two muons should form a common vertex and have a combined invariant mass between 2.8 and  $3.35 \text{ GeV}/c^2$ .

An additional charged particle with  $p_T > 0.5 \text{ GeV}/c$ , with total momentum above  $0.7 \text{ GeV}/c$ , and with at least 2 measurements in SMT was selected. This particle was assigned the kaon mass. It was required to have a common vertex with the two muons with  $\chi^2 < 16$  per 3 degrees of freedom. The displacement of this vertex from the primary interaction point was required to exceed 3 standard deviations in the plane perpendicular to the beam direction.

From each set of three particles fulfilling these requirements, a  $B^+$  candidate was constructed. The momenta of muons were corrected using the  $J/\psi$  mass constraint. The track of the  $B^+$  was assumed to pass through the reconstructed vertex and to be directed along its momentum. The reconstructed track of the  $B^+$  was used to determine the axial [17]  $\epsilon_T$  and stereo [18]  $\epsilon_L$  projections of its track impact parameter with respect to the primary vertex together with the corresponding errors ( $\sigma(\epsilon_T)$ ,  $\sigma(\epsilon_L)$ ). Since the  $B^+$  track should originate from the primary vertex, the combined significance  $S_B$ , defined as:

$$S_B = (\epsilon_T/\sigma(\epsilon_T))^2 + (\epsilon_L/\sigma(\epsilon_L))^2 \quad (4)$$

was required to be less than 40.

The obtained event samples were used to construct the final selection of  $B^+ \rightarrow J/\psi K^+$  using the likelihood ratio method, described below. It is assumed that a set of discriminating variables  $x_1, \dots, x_n$  can be constructed for a given event. It is also assumed that probability density functions  $f^s(x_i)$  for the signal and  $f^b(x_i)$  for the background can be built for each variable  $x_i$ . The combined tagging variable  $y$  is defined as:

$$y = \prod_{i=1}^n y_i; \quad y_i = \frac{f_i^b(x_i)}{f_i^s(x_i)} \quad (5)$$

A given variable  $x_i$  can be undefined for some events. In this case, the corresponding variable  $y_i$  is set to 1. The selection of the signal is obtained by applying a cut  $y < y_0$ .

The following discriminating variables were used:

- Transverse momentum of the kaon;
- Minimal transverse momentum of the two muons;
- $\chi^2$  of the  $B^+$  decay vertex;
- $B^+$  decay length divided by its error;
- Combined significance of the  $B^+$  defined in (4);
- Combined significance of the kaon with respect to the primary vertex defined similarly to (4).

The probability density functions for both signal and background were obtained from data. The signal was defined by all events with  $5.19 < M(\mu^+\mu^-K^+) < 5.34 \text{ GeV}/c^2$ , and the background was defined by those events with  $4.98 < M(\mu^+\mu^-K^+) < 5.13 \text{ GeV}/c^2$  or  $5.40 < M(\mu^+\mu^-K^+) < 5.55 \text{ GeV}/c^2$ . The background probability density function for each variable was constructed using the sum of events in the two background bands. The signal probability density function was constructed by subtracting the average of the two sidebands from the distribution of events in the signal band. Fig. 1 shows the distribution of the combined tagging variable defined by equation (5). For the final selection of  $B^+ \rightarrow J/\psi K^+$  decays, the cut  $\log_{10} y < -0.08$  was applied. With this cut the ratio  $N(\text{signal})/\sqrt{N(\text{tot})}$  is very close to the maximal value. The resulting mass distribution of the  $J/\psi K^+$  system in data is shown in Fig. 2. The signal peak corresponding to the decay  $B^+ \rightarrow J/\psi K^+$  contains  $16219 \pm 180$  events.

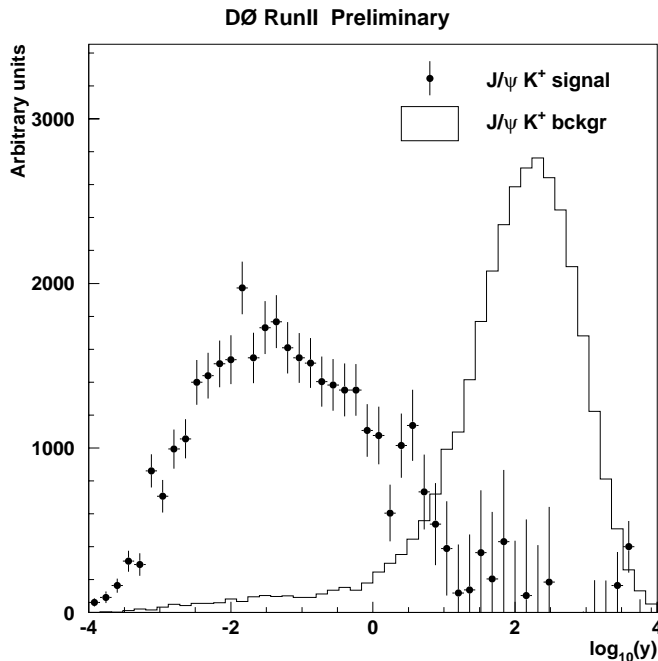


FIG. 1: Distributions of  $\log_{10}(y)$  where  $y$  is a combined tagging variable defined by (5).

## 2.2. $B_J$ Selection

The obtained sample of  $B$  hadrons was used to select the  $B_J \rightarrow B^{(*)}\pi$  decay. For each reconstructed  $B$  hadron candidate, an additional track, passing the following criteria, was selected:

- $\geq 2$  hits in both SMT and CFT;

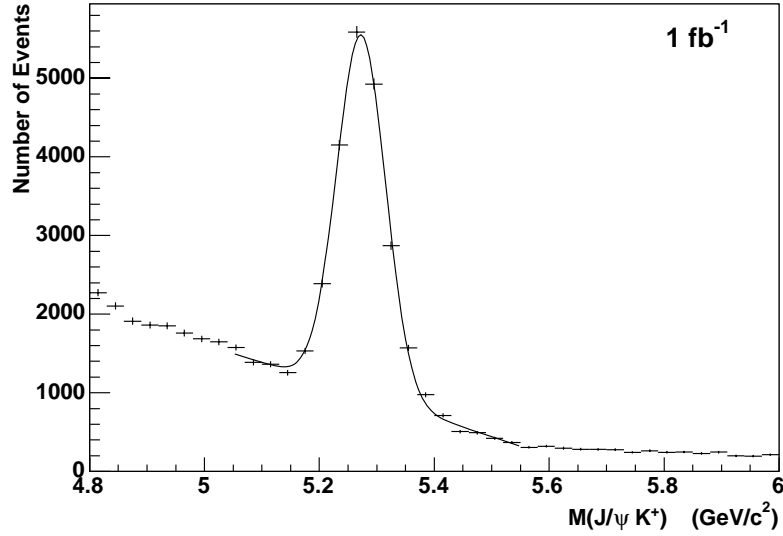


FIG. 2: Mass distribution of  $J/\psi K^+$  events. The curve shows the fit by the sum of a Gaussian describing the signal  $B^+ \rightarrow J/\psi K^+$  and polynomial background.

- Transverse momentum  $\geq 0.75$  GeV/c;
- Correct charge correlation ( $B^+ \pi^-$  or  $B^- \pi^+$ );

Since  $B_J$  decays at the production point, the additional track was required to originate from the primary interaction point by applying the condition on its combined significance  $S_\pi < 6$ , where  $S_\pi$  was defined similarly to (4) using the impact parameters of the pion. Only those  $B^+$  mesons with a mass  $5.19 < M(B^+) < 5.36$  were selected to reconstruct the  $B_J$  candidates. This is the  $2\sigma$  mass window around the  $B^+$  peak.

For each track combination satisfying the above criteria, the mass difference  $\Delta M = M(B\pi) - M(B)$  was computed. The resulting distribution of the  $\Delta M$  is shown in Fig. 3. The signal exhibits a three peak structure, which is interpreted in terms of the decay modes  $B_J \rightarrow B^{+(*)}\pi$ . The highest mass peak (at  $\sim 470$  MeV/ $c^2$ ) corresponds to  $B_2^* \rightarrow B^+\pi$ . The  $B_2^*$  meson can also decay via the process  $B_2^{*0} \rightarrow B^{*+}\pi$ , where the  $B^{*+}$  then decays to  $B^+\gamma$  with 100 % probability. The photon released in this process has an energy of  $45.78 \pm 0.35$  MeV/ $c^2$  [1]. In this analysis, the photon is not reconstructed, and therefore  $B_2^* \rightarrow B^{*+}\pi$  is observed as a second peak separated from the direct peak by the mass difference  $\Delta M$ :

$$\Delta M = M(B\pi) - M(B) \simeq M(B\pi\gamma) - M(B\gamma) = M(B_J) - M(B^*). \quad (6)$$

This is observed in Fig. 3 as the structure at  $\sim 420$  MeV/ $c^2$ . The branching ratio of  $B_2^*$  to  $B^*\pi$  and  $B\pi$  predicted by theory is 1:1. The direct decay  $B_1 \rightarrow B\pi$  is forbidden by angular momentum and parity conservation, and so only the decay  $B_1 \rightarrow B^{*+}\pi$  is observed. The non-reconstructed photon in the resulting decay of  $B^{*+}$  leads to a mass peak displaced downwards from the true mass of the  $B_1$  by  $\sim 46$  MeV/ $c^2$ . This is the lowest mass peak in Fig. 3, at  $\sim 395$  MeV/ $c^2$ .

The mass resolutions were studied using Monte Carlo simulated data. The standard DØ software, i.e. the EvtGen [13] generator interfaced to PYTHIA[14] and followed by the full GEANT modelling of the detector response and event reconstruction, was used for the simulations. All three decays  $B_1^0 \rightarrow B^{*+}\pi$ ,  $B_2^{*0} \rightarrow B^{*+}\pi$  and  $B_2^{*0} \rightarrow B\pi$  were generated. The mass resolutions for  $B_J \rightarrow B^*\pi$  and  $B_J \rightarrow B\pi$  were found to be consistent for all three decays.

With this taken into account, the expected  $\Delta M$  distribution has three peaks with the central positions:

- $\Delta_1 = M(B_1) - M(B^*)$ , corresponding to the decay  $B_1 \rightarrow B^*\pi$ ;
- $\Delta_2 = M(B_2^*) - M(B^*)$ , corresponding to  $B_2^* \rightarrow B^*\pi$ ;
- $\Delta_3 = M(B_2^*) - M(B)$ , corresponding to  $B_2^* \rightarrow B\pi$ ;

In addition to these narrow  $P$  states, there should be two wide  $B_J$  states decaying to  $B^{+(*)}\pi$  through the  $S$ -wave. However, all theoretical models [2–5] predict their width to be large, up to 1 GeV/ $c^2$ , so that they cannot be distinguished from the non-resonant background with the current statistics.

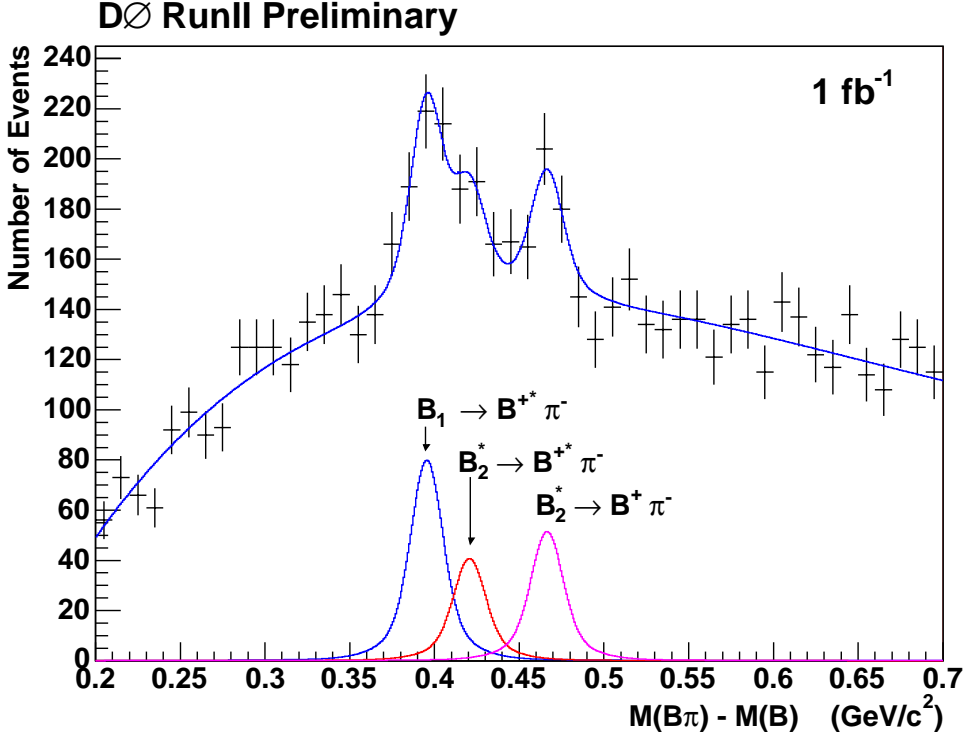


FIG. 3: Mass difference  $\Delta M = M(B\pi) - M(B)$  for exclusive  $B$  decays. The line shows the fit by the function (7). The contribution of background and the three signal peaks are shown separately.

Following this expected pattern, the experimental distribution was fitted by the following function:

$$F(\Delta M) = F_{sig}(\Delta M) + F_{back}(\Delta M)$$

$$F_{sig}(\Delta M) = N \cdot (f_1 \cdot G(\Delta M, \Delta_1, \Gamma_1) + (1 - f_1) \cdot (f_2 \cdot G(\Delta M, \Delta_2, \Gamma_2) + (1 - f_2) \cdot G(\Delta M, \Delta_3, \Gamma_2))). \quad (7)$$

In these equations,  $\Gamma_1$  and  $\Gamma_2$  are the widths of  $B_1$  and  $B_2^*$ ,  $f_1$  is the fraction of  $B_1$  contained in the  $B_J$  signal and  $f_2$  is the fraction of  $B_2^* \rightarrow B^* \pi$  decay in  $B_2^{*0}$  signal. The parameter  $N$  gives the total number of observed  $B_J \rightarrow B^{(*)} \pi$  decays. The background  $F_{back}(\Delta M)$  was parameterized by a fourth-order polynomial.

The function  $G(x, x_0, \Gamma)$  is the convolution of the relativistic Breit-Wigner function with the experimental resolution in  $\Delta M$  (parameterized by the double Gaussian function calculated from simulation):

$$G(x, x_0, \Gamma_0) = \frac{1}{N_0} \int Res(\sigma_1, \sigma_2, x', x, S) \cdot \frac{x_0 \Gamma(x)}{(x'^2 - x_0^2)^2 + x_0^2 \Gamma^2(x)} dx' \quad (8)$$

$$Res(\sigma_1, \sigma_2, x, \hat{x}, S) = \frac{1}{\sqrt{2\pi}\sigma_1} \cdot \frac{1}{S+1} \exp\left(-\frac{(x - \hat{x})^2}{2\sigma_1^2}\right) + \frac{1}{\sqrt{2\pi}\sigma_2} \cdot \frac{S}{S+1} \exp\left(-\frac{(x - \hat{x})^2}{2\sigma_2^2}\right) \quad (9)$$

$$N_0 = \int \frac{x_0 \Gamma(x)}{(x^2 - x_0^2)^2 + x_0^2 \Gamma^2(x)} dx \quad (10)$$

$$\Gamma(x) = \Gamma_0 \frac{x_0}{x} \left(\frac{k}{k_0}\right)^{2L+1} F^{(L)}(k, k_0) \quad (L = 2) \quad (11)$$

$$F^{(2)}(k, k_0) = \frac{9 + 3(k_0 r)^2 + (k_0 r)^4}{9 + 3(kr)^2 + (kr)^4} \quad (12)$$

The variables  $k, k_0$  in (11-12) are the magnitude of the pion three-momentum in the  $B_J$  rest frame when  $B_J$  has a four-momentum-square equal to  $x^2$  and  $x_0^2$  respectively,  $F^{(2)}(k, k_0)$  is the Blatt-Weiskopf form factor for  $L = 2$  decay [15] and  $r = 5 \text{ (GeV/c)}^{-1}$  is a B hadron mass scale. The widths  $\sigma_1$  and  $\sigma_2$ , and the scale parameter  $S$ , are fixed from the simulation.

All theoretical models predict that the widths  $\Gamma_1$  and  $\Gamma_2$  of  $B_1$  and  $B_2^*$  are almost equal. Therefore, they were set to be equal in the fit:  $\Gamma_1 = \Gamma_2 = \Gamma$ . In addition, the mass difference of  $B^*$  and  $B^+$  was fixed at the PDG value of

TABLE I: The correlation coefficients between fitted parameters

parameter	$N$	$f_1$	$f_2$	$M(B_1)$	$M(B_2^*) - M(B_1)$	$\Gamma$
$N$	1.000	-0.028	-0.080	-0.196	0.136	0.668
$f_1$	-0.028	1.000	-0.348	0.329	-0.143	0.236
$f_2$	-0.080	-0.348	1.000	-0.313	0.266	-0.167
$M(B_1)$	-0.196	0.329	-0.313	1.000	-0.636	-0.076
$M(B_2^*) - M(B_1)$	0.136	-0.143	0.266	-0.636	1.000	-0.035
$\Gamma$	0.668	0.236	-0.167	0.076	-0.035	1.000

45.78 MeV/c<sup>2</sup> [1]. With these assumptions, the following parameters of  $B_1$  and  $B_2^*$  were obtained:

$$N = 504 \pm 80 \text{ events} \quad (13)$$

$$M(B_1) - M(B^+) = 441.3 \pm 2.5 \text{ MeV}/c^2 \quad (14)$$

$$M(B_2^*) - M(B_1) = 25.2 \pm 3.0 \text{ MeV}/c^2 \quad (15)$$

$$\Gamma = \Gamma_1 = \Gamma_2 = 6.6 \pm 5.3 \text{ MeV}/c^2 \quad (16)$$

$$f_1 = 0.464 \pm 0.064 \quad (17)$$

$$f_2 = 0.442 \pm 0.092 \quad (18)$$

$$\chi^2/NDF = 62.4/69 \quad (19)$$

The errors given are statistical only. Without the  $B_J$  signal contribution, the  $\chi^2$  of the fit is increased by 79, which implies that this structure has been observed with a statistical significance of more than  $\sim 7\sigma$ . Fitting with only one peak increases the  $\chi^2$  by 20. Table I gives the correlation coefficients between the fitted parameters.

### 3. $B_J$ RELATIVE PRODUCTION RATE

The observed number of  $B_J$  mesons was used to measure the production rate  $Br(b \rightarrow B_J \rightarrow B^+\pi^-)/Br(b \rightarrow B^+)$ . In this ratio many uncertainties of the  $B^+$  reconstruction efficiency cancel or decrease, which, in particular, allows the use of events selected by all triggers. The efficiency to select an additional pion from  $B_J$  decay was determined from a dedicated simulation. A sample of  $\sim 22,000$   $B_J$  events was generated, with the particle parameters (masses, widths, decay fraction of  $B_2^*$ ) selected to be consistent with the values measured from the data analysis detailed in section 2. The  $B^+$  particles were decayed entirely to the  $J/\psi K^+$  final state.

The efficiency for each decay mode (1-3) was computed separately, to take into account small variations from channel to channel:

$$\varepsilon(B_1 \rightarrow B^{*+}\pi)/\varepsilon(B^+) = 28.2 \pm 0.8\% \quad (20)$$

$$\varepsilon(B_2 \rightarrow B^{*+}\pi)/\varepsilon(B^+) = 30.5 \pm 0.8\%$$

$$\varepsilon(B_2 \rightarrow B^+\pi)/\varepsilon(B^+) = 35.5 \pm 0.8\%$$

The uncertainty given for these values comes from the limited simulation statistics. The associated systematic uncertainty is discussed in section 4. Using these efficiencies and the values  $f_1, f_2$  from the fit, we obtain:

$$R_1 = \frac{Br(B_1 \rightarrow B^{*+}\pi)}{Br(B_J \rightarrow B^{(*)}\pi)} = 0.545 \pm 0.064 \text{ (stat)} \quad (21)$$

$$R_2 = \frac{Br(B_2^{*0} \rightarrow B^*\pi)}{Br(B_2^{*0} \rightarrow B^{(*)}\pi)} = 0.513 \pm 0.092 \text{ (stat)} \quad (22)$$

The systematic errors associated with these values are discussed in section 4.

The obtained values are used to calculate the relative production rate as follows. The  $B^+$  mass signal in data contains  $16219 \pm 180$  events, of which only those in the central  $\pm 2\sigma = \pm 85$  MeV/c<sup>2</sup> mass window ( $5.19 \rightarrow 5.36$  GeV/c<sup>2</sup>) are used in the reconstruction of  $B_J$ . Applying the statistical factor 0.9545 to account for this mass window,  $15481 \pm 172$   $B^+$  mesons are detected. There are  $504 \pm 80$   $B_J$  mesons detected from the same sample. The production

TABLE II: Systematic uncertainties of  $B_J$  parameters

source	$dM(B_1)$ (MeV/c <sup>2</sup> )	$d(M(B_2^*) - M(B_1))$ (MeV/c <sup>2</sup> )	$d\Gamma_{1,2}$ (MeV/c <sup>2</sup> )	$dR_1$	$dR_2$	N
Background parameterization	0.8	0.3	3.4	0.012	0.01	64
Fitting range	0.2	0.2	1.0	0.008	0.01	22
Bin widths/positions	5.2	0.9	n/a	0.069	0.114	18
$\Gamma_2$ free in the fit	0.2	0.1	2.1	n/a	n/a	2
$B^{+*}$ mass uncertainty	0.3	0.2	0.04	0.002	0.002	0
$\sigma(\Delta M) \pm 28\%$	0.2	0.3	0.75	0.007	0.008	10
Momentum scale	0.5	0.03	0	0	0	0
Total	5.30	1.04	4.2	0.071	0.115	71

rate ratio is then calculated thus:

$$\begin{aligned}
\frac{R(b \rightarrow B_J^0 \rightarrow B^{(*)+}\pi^-)}{R(b \rightarrow B^+)} &= \frac{N(B_J) f_1}{N(B^+)} \frac{\varepsilon(B^+)}{\varepsilon(B_1 \rightarrow B^{+*}\pi)} \\
&+ \frac{N(B_J) (1 - f_1) f_2}{N(B^+)} \frac{\varepsilon(B^+)}{\varepsilon(B_2 \rightarrow B^{+*}\pi)} \\
&+ \frac{N(B_J) (1 - f_1) (1 - f_2)}{N(B^+)} \frac{\varepsilon(B^+)}{\varepsilon(B_2 \rightarrow B^+\pi)} \\
&= 0.110 \pm 0.016 \text{ (stat)}
\end{aligned} \tag{23}$$

Due to isospin conservation, the neutral pion final states of the  $B_J$  have  $\text{Br}(B_J^0 \rightarrow B^{(*)+}\pi^-) = 2 \text{Br}(B_J^0 \rightarrow B^{(*)0}\pi^0)$ . Therefore, the total rate of  $B_J$  meson production was found to be:

$$R_J = \frac{\text{Br}(b \rightarrow B_J^0 \rightarrow B^{(*)}\pi)}{\text{Br}(b \rightarrow B^+)} = 0.165 \pm 0.024 \text{ (stat)} \tag{24}$$

#### 4. SYSTEMATIC ERRORS AND CONSISTENCY CHECKS

The influence of different sources of systematic uncertainty was estimated as follows. Different background parameterizations (polynomials of 3rd, 4th and 5th order) were used in the fit on the  $\Delta M$  distribution. The fitting range of this distribution was varied. The parameters describing the background were allowed to vary in the fit and their error was already included in (13-19). To check the effect of assumption  $\Gamma_1 = \Gamma_2$ , the widths  $\Gamma_1$  and  $\Gamma_2$  were allowed to vary independently in the fit. This yielded values  $\Gamma_1 = 7.8 \pm 5.0 \text{ MeV}/c^2$ ,  $\Gamma_2 = 4.5 \pm 5.0 \text{ MeV}/c^2$ , and the change in parameters was taken as the systematic error from this source. The effect of the uncertainty on the mass difference  $M(B^{+*}) - M(B^+)$  [1] was also taken into account. In addition, since a binned-fit was used, the effect of bin widths and positions was tested by varying over a range of binning schemes.

The detector mass resolution (the high- $\sigma$  part of the double-Gaussian parameterization) was varied by 28%, which corresponds to the difference between the data and simulation in the measured width of the mass difference  $M(D^{*+}) - M(D^0)$ . The measured mass of  $B^+$  is shifted down relative to the world average value due to an uncertainty in the  $D\bar{O}$  momentum scale by  $\sim 6 \text{ MeV}/c^2$ . The mass differences  $M(B_1) - M(B^*)$  and  $M(B_2^*) - M(B_1)$  were corrected by the ratio of the measured and accepted mass of  $B$ -hadron and 100% uncertainty was assigned to this mass scale correction. The summary of all systematic errors is given in Table II. In addition, the fit was repeated without the Blatt-Weiskopf form-factor (12) and no visible change in results was observed.

The additional systematic uncertainties of the  $B_J$  production rate were computed as follows. To test for systematic uncertainty on the  $B^+$  signal size, different background parameterizations were used for the fit. The range of the fit was also varied. The resulting uncertainty in the number of  $B^+$  events is 121 events. The systematic error on the  $B_J$  signal size is calculated in Table II. The difference in the impact parameter resolution between data and simulation was estimated to be  $\sim 10\%$ . It can influence the measurement of the selection efficiency of the pion from  $B_J$  decay. Since the value of  $S_\pi$  used to select this pion is proportional to the square of the impact parameter, the cut on  $S_\pi$  was varied by 20%. This resulted in a variation of the  $\varepsilon(B_J)/\varepsilon(B)$  by 0.03. The track reconstruction efficiency for particles with low transverse momentum was measured in [16] and a good agreement between data and simulation was found. This comparison is valid within the uncertainties of branching ratios of different  $B$  semileptonic decays, which is about 7%. This systematic uncertainty is assigned to all measured ratios of efficiency (20). An additional systematic uncertainty associated to the difference in the momentum distribution of selected particles in data and in

simulation was taken into account. All systematic uncertainties in the  $B_J$  production rate are summarized in Table III. Combining in quadrature all these effects, the total systematic error in the relative production rate (24) was found to be 0.028.

TABLE III: Systematic uncertainties of relative  $B_J$  production rate

source	$d(R_J)$
Number of $B_J$ events	0.023
Number of $B^+$ events	0.001
Momentum difference	0.007
Uncertainty in resolution	0.015
$\pi$ reconstruction efficiency	0.004
Total	0.028

Different consistency checks of the observed signal were performed. The events with positively and negatively charged pions were analyzed separately. The result of the fit is shown in Fig. 4 The complementary sample of events containing the pion not compatible with the primary vertex was selected by requiring  $S_\pi > 16$ . No significant signal of  $B_J$  was observed, as can be seen in Fig. 5. Events with wrong charge combinations ( $B^+\pi^+$  and  $B^-\pi^-$ ) also showed a signal consistent with zero, as observed in Fig. 6. The stability of the fit under different selections was verified over variations in  $P_T^{min}$ ,  $(S_{PV}^2)^{max}$  and the width of the  $B^+$  mass window.

## 5. CONCLUSIONS

In conclusion, the  $B_1$  and  $B_2^*$  are observed for the first time as two separate objects. Their masses and the average width were measured to be:

$$M(B_1) = 5720.8 \pm 2.5 \text{ (stat)} \pm 5.3 \text{ (syst)} \text{ MeV}/c^2 \quad (25)$$

$$M(B_2^*) - M(B_1) = 25.2 \pm 3.0 \text{ (stat)} \pm 1.1 \text{ (syst)} \text{ MeV}/c^2 \quad (26)$$

The width of both  $B_1^0$  and  $B_2^{*0}$  mesons was set to be equal in this analysis, and with this assumption was found to be:

$$\Gamma_1 = \Gamma_2 = 6.6 \pm 5.3 \text{ (stat)} \pm 4.2 \text{ (syst)} \text{ MeV}/c^2 \quad (27)$$

The branching ratio of  $B_2^*$  to the excited state  $B^*$  was measured as:

$$\frac{Br(B_2^* \rightarrow B^* \pi)}{Br(B_2^* \rightarrow B^{(*)} \pi)} = 0.513 \pm 0.092 \text{ (stat)} \pm 0.115 \text{ (syst)} \quad (28)$$

The composition of the  $B_J$  sample was measured. The fraction in the state  $B_1$  was measured as:

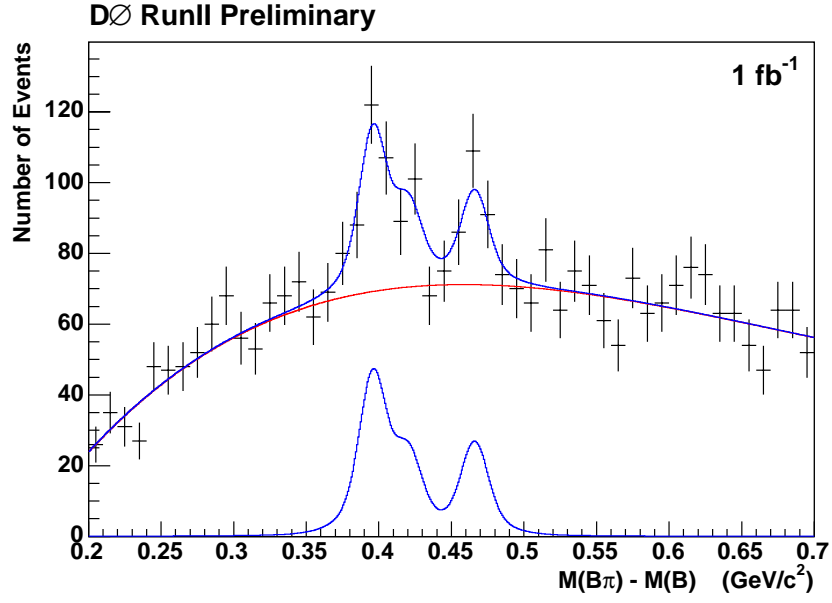
$$\frac{Br(B_1 \rightarrow B^{*+} \pi)}{Br(B_J \rightarrow B^{(*)} \pi)} = 0.545 \pm 0.064 \text{ (stat)} \pm 0.071 \text{ (syst)} \quad (29)$$

The  $B_J$  production rate is measured as a fraction of the  $B^+$  production rate:

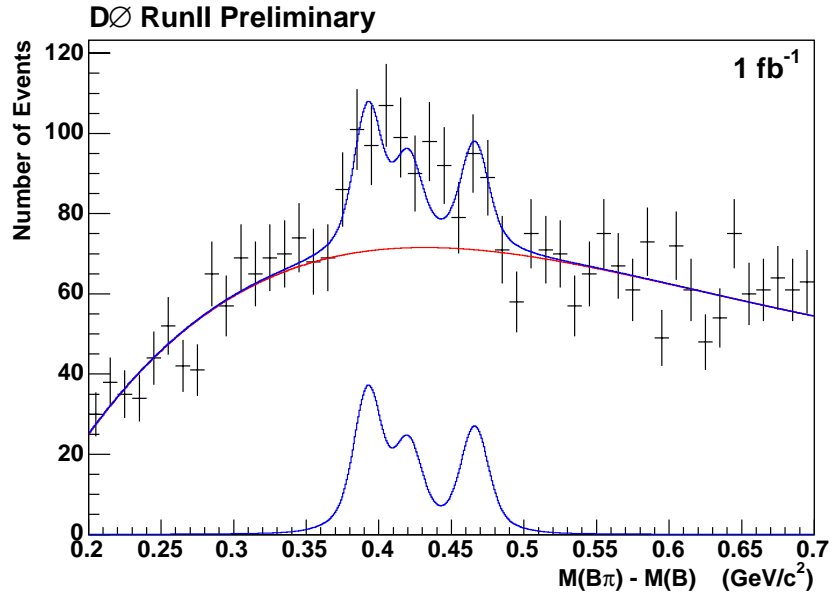
$$\frac{Br(b \rightarrow B_J^0 \rightarrow B\pi)}{Br(b \rightarrow B^+)} = 0.165 \pm 0.024 \text{ (stat)} \pm 0.028 \text{ (syst)} \quad (30)$$

- 
- [1] S.Eidelman *et al.* (Particle Data Group), Phys. Lett. **B592**, 1 (2004).  
[2] M. Di Pierro and E. Eichten, Phys. Rev. D **64** (2001) 114004 [arXiv:hep-ph/0104208].  
E.J.Eichten, C.T.Hill, C.Quigg, Phys. Rev. Lett. **71**, 4116 (1993) and an update FERMILAB-CONF-94/118-T.  
[3] N.Isgur, Phys. Rev. **D57**, 4041 (1998).  
[4] D.Ebert, V.O.Galkin, R.N.Faustov, Phys. Rev. **D57**, 5663 (1998), Erratum Phys. Rev. **D59** 019902 (1999).  
[5] A.H.Orsland, H.Hogaasen, Eur.Phys.J. **C9** 503 (1999).

- [6] OPAL Collab., Z. Phys. **C66**, 19 (1995).
- [7] DELPHI Collab., Phys. Lett. **B345**, 598 (1995).
- [8] ALEPH Collab., Z. phys. **C69**, 393 (1996).
- [9] CDF Collab., Phys. Rev. **D64**, 072002 (2001).
- [10] ALEPH Collab., Phys. Lett. **B425**, 215 (1998).
- [11] Charge conjugated states are always implied.
- [12] V.M. Abazov *et al.* (DØ collaboration), “The Upgraded DØ Detector” [arXiv:hep-physics/0507191]
- [13] D.J.Lange, Nucl. Instrum. Meth. **A462**, 152 (2001).
- [14] T.Sjöstrand *et. al.* hep-ph/0108264
- [15] J.Blatt and V.Weisskopf, Theoretical Nuclear Physics, p.361, New York: John Wiley & Sons (1952).
- [16] V.M. Abazov *et al.* (DØ collaboration), Phys. Rev. Lett. **94**, 182001 (2005).
- [17] in the plane perpendicular to the beam direction
- [18] parallel to the beam direction



(a) Positive Pion



(b) Negative Pion

FIG. 4: Mass difference  $\Delta M = M(B\pi) - M(B)$  for events with positive pion (upper plot) and negative pion (lower plot). The line shows the fit by the function (7). The contributions of the background and signal are shown separately.

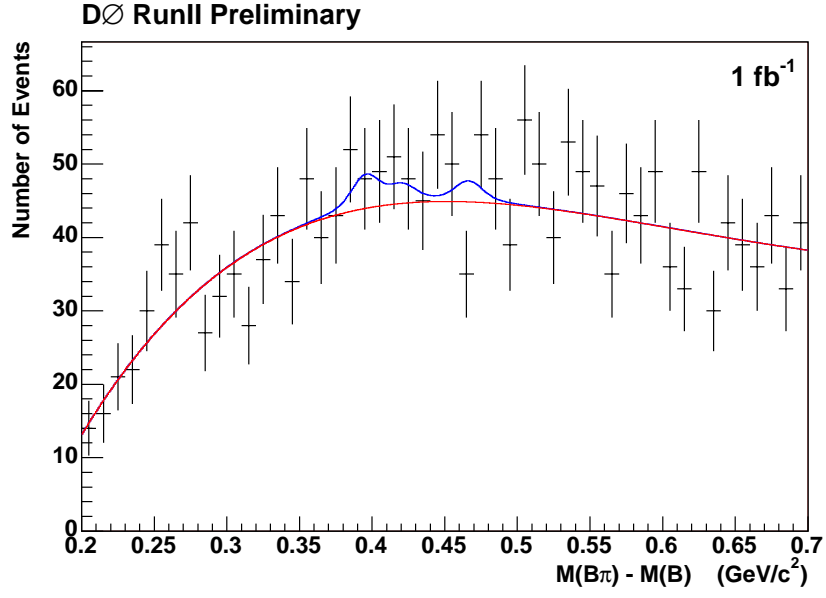


FIG. 5: Mass difference  $\Delta M = M(B\pi) - M(B)$  for events with the pion not compatible with the primary vertex ( $S_{PV}^2 > 16$ ). The line shows the fit by the function (7) with and without the  $B_J$  signal.

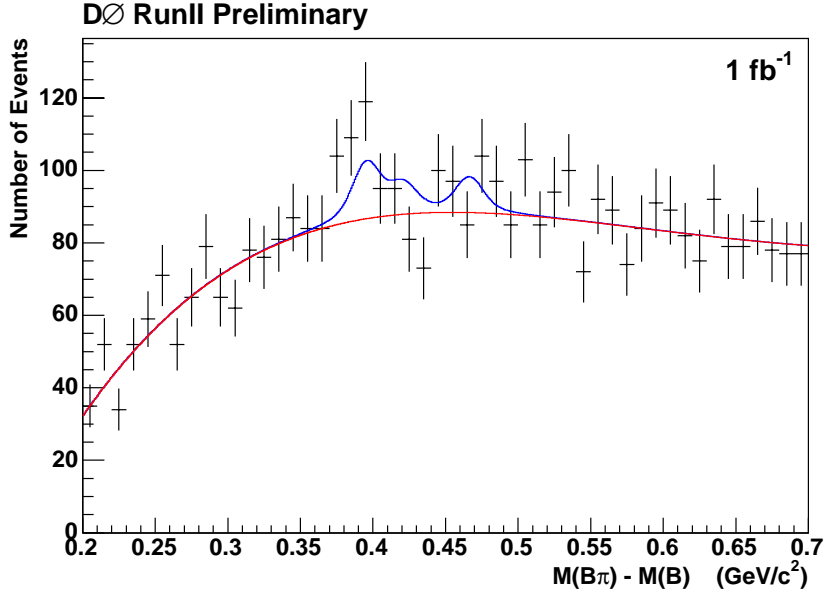


FIG. 6: Mass difference  $\Delta M = M(B\pi) - M(B)$  for events with wrong charge combinations ( $B^+\pi^+$  and  $B^-\pi^-$ ). The line shows the fit by the function (7) with and without the  $B_J$  signal. The signal parameters are fixed at the values found in opposite charge events. Without fixing these parameters the peak positions, widths and heights change significantly from those found in data.